Meso-scale Modeling of Static and Fatigue Damage in Woven Composite Materials with Finite Element Method

J. Xu[a*], SV. Lomov[a], I. Verpoest[a], S. Daggumati [b], W. Van Paepegem[b], J. Degrieck[b]

[a]Katholieke Universiteit Leuven, Department of Metallurgy and Materials Engineering, Kasteelpark Arenberg 44 B-3001 Leuven, Belgium

[b]Ghent University, Dept. of Materials Science and Engineering, Sint-Pietersnieuwstraat 41, 9000 Gent, Belgium

Email: Jian.Xu@mtm.kuleuven.be

SUMMARY

Aim of this work is to evaluate the fatigue damage in textile composites on meso-scale level. Pre-damage properties, damage thresholds and damage propagation of unit cell (UC) are calculated and validated by experiments. Quasi-static damage algorithm is further used to model the cycles of the fatigue loading. Model output is the computed S-N curve of textile composites.

Keywords: meso-scale; woven composite; fatigue damage; finite elements; stiffness degradation method; multi-axial fatigue

1. INTRODUCTION

Textile reinforced composites are increasingly applied to many industrial fields, for instance automotive, aerospace and new energy. Fatigue design criteria of those materials are usually determined by experiments. However, due to the complex and variable architectures and design parameters of the reinforcement and considerable time consumption of the tests, a reliable numerical method for evaluation of the fatigue strengths (presented in S-N curve) would be of great value.

Methodology of this modeling work is: (a) Meso-FE model of a textile composite is considered, with the material of the impregnated yarns represented with homogenized properties of UD fibre reinforced composite with a local fibre volume fraction [3]; (b) Stiffness degradation method [4] is employed as stiffness reductive models both in static and fatigue damage evaluation; (c) Fibre fatigue damage and inter-fibre fatigue damage are considered as independent fatigue loading modes and the concept of multi-axial fatigue is applied for the inter-fibre fatigue; (d) When the UC is loaded to maximum fatigue load, static damage is taken into account as well as the stress redistribution after fatigue damage. Some aspects of this approach were previously reported in [1,2].

Averaged stiffness, Poisson ratios of pre- and post damage phase are calculated based on numerical homogenization technique with periodic boundary conditions (PBCs). The damage accumulation and stiffness degradation model are implemented into Abaqus user defined material subroutine (UMAT). Complete fatigue data for carbon fibre epoxy (AS4/3501-6) UD composites with fibre volume fraction (Vf) at 62% was obtained by Shokrieh [5]. Those sets of experimental data are processed to produce the S-N curves used as input for the calculation reported here. For validation of the modeling, experimental data of plain weave carbon fibre reinforced composite (PW12K-CFRP), published in [6], is used. The computed S-N curve shows agreement with the experimental data for tension fatigue of PW12K-CFRP.

2. FATIGUE MODELING

2.1 The Overall Algorithm

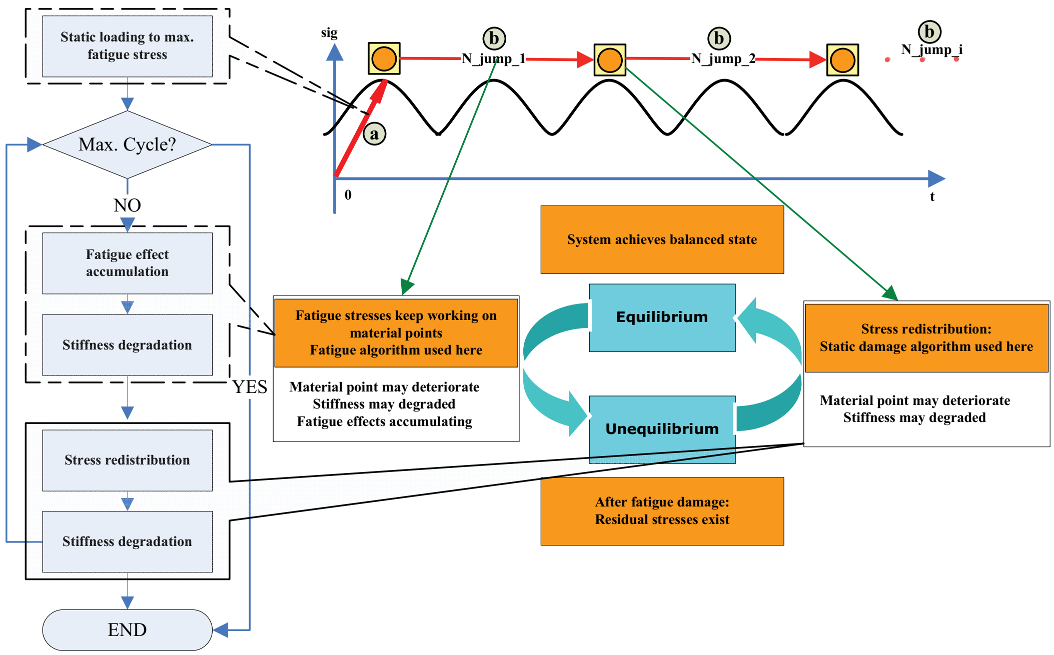

Fig.1 Sketch map of the algorithm of fatigue analysis of textile composites

The approach to predict fatigue damage could be divided into two stages – Fig.1: (a) Static loading is applied to UC gradually up to the magnitude of maximum fatigue loading. During this stage, some of the material points are identified as damaged and their stiffness is degraded. The degraded properties will be passed to fatigue analysis later --a in Fig.1. (b) Fatigue damage analysis stage could again be divided into two sub-procedures: (**i**) Local fatigue stresses wear out the material points. During certain amount of load cycles (N_jump), materials points continuously experience the weakening effects from the stresses in local coordinates system – b in Fig.1. Some of them are identified as damaged in fatigue and their stiffness is degraded by means of anisotropic damage model – Table.2. The rest of them do not reach the critical moment and those points will keep there stiffness intact. However, the fatigue effect historically applied on those un-deteriorated material points must be “recorded”. Hence, at the end of next N_jump, all the previous fatigue effects plus the newest weakening effects will be added together and evaluated for fatigue damage by Miner’s rule. (**ii**) Residual stresses release (stress redistribution). After the deterioration of certain amount of material points in UC, the model shows un-equilibrium due to local residual stresses. To re-achieve the equilibrium state, the FE-model will adjust itself by employing the static damage algorithm. Sequences of the stress redistribution could be that new material deterioration occurs around previously damaged points – the widening of damage zone.

In the current version of the tool, *N_jump* is kept constant. Results show good convergence with different constant “distances” of *N_jump*. An alternative is to use the auto-calculated *N_jump*, which means that the program will evaluate the next *N_jump* before each fatigue damage analysis (real-time calculation).

The two key components of the fatigue modeling algorithm of Fig. 1 are the multi-axial fatigue damage model of UD reinforced composite, applied in the Gaussian points , and quasi-static damage analysis of the UC, used to determine “additional” damage in the individual fatigue cycle after *N_jump* and to recalculate the equilibrium. These two key points are explained in the subsequent sections.

2.2 Fatigue Damage Initiation for UD Composite: Multi-axial Fatigue

Most of the critical mechanical parts experience multi-axial cyclic loadings during the service time. For anisotropic material, such as textile composites, even under external uni-axial fatigue loading, locally it is multi-axially fatigued. Other possible reasons are, for example, the complex loading history or various cracks orientations after damage initiation.

Although there are numerous proposed models in reports, most of them are limited by specific material or loading conditions [7] or can not predict the crack orientation, which is a crucial parameter for anisotropic damage mode. In the paper [7], Liu proposed a new mode based on “critical plane” theory, which depends on the “crack plane” (plane with the maximum stress) and materials properties. In his later paper [8], Liu extended the model to anisotropic materials. In Eq.1, to meet the requirement of 3D stress state in yarn, new term representing out-of-plane shear ($\tau_{a,c(3)}$) is added. When Eq.1 is satisfied, the simulation tool considers a local fatigue failure in material point.

$$\frac{1}{\beta}\sqrt{\left[\sigma_{a,c(1)}^{2}\left(1+\eta_{N_f}\frac{\sigma_{m,c(1)}^{2}}{f_{N_f(\theta_{\max})}}\right)\right]^{2}+\left(\frac{f_{N_f(\theta_{\max})}}{t_{N_f(\theta_{\max})(2)}}\right)\left(\tau_{a,c(2)}\right)^{2}+\left(\frac{f_{N_f(\theta_{\max})}}{t_{N_f(\theta_{\max})(3)}}\right)\left(\tau_{a,c(3)}\right)^{2}+k\left(\sigma_{a,c}^{H}\right)^{2}}=f_{N_f(\theta_{\max})} \qquad (1)$$

In Eq.1, $\sigma_{a,c(1)}$, $\sigma_{m,c(1)}$, $\sigma_{a,c}^{H}$, $\tau_{a,c(2)}$ and $\tau_{a,c(3)}$ stand for normal stress, mean normal stress, hydrostatic stress, in-plane shear stress and out-of-plane-shear stress amplitudes on critical plane, respectively. β, k and α are material properties related constants and angle between crack plane and critical plane, which are defined in Table.1. η_{N_f} describes the effect of mean normal stress, which is experimentally curve-fitted. $f_{N_f(\theta_{\max})}$, $t_{N_f(\theta_{\max})(2)}$ and $t_{N_f(\theta_{\max})(3)}$ are fatigue strengths on crack plane, which are tensile fatigue strength, in-plane shear and out-of-plane-shear strength, respectively. $\theta_{\max}$ is the angle between norm of crack plane and fibre direction. Crack plane is the micro plane which has physical crack. According to Model II crack theory, crack plane experiences the largest norm stress. Fatigue strengths on crack plane, which are functions of angle $\theta_{\max}$, can be calculated through Tsai-Wu strength transformation.

Table 1. Material constants for multi-axial fatigue damage evaluation [7]

Material constants	$s = t_{N_f(\theta_{max})(2)} / f_{N_f(\theta_{max})} \leq 1$	$s = t_{N_f(\theta_{max})(2)} / f_{N_f(\theta_{max})} > 1$
α	$\cos(2\alpha) = -2 + \sqrt{4 - 4(1/s^2 - 3)(5 - 1/s^2 - 4s^2)} / 2(5 - 1/s^2 - 4s^2)$	$\alpha = 0$
k	$k = 0$	$k = 9(s^2 - 1)$
β	$\beta = [\cos^2(2\alpha)s^2 + \sin^2(2\alpha)]^{0.5}$	$\beta = s$

The steps to evaluate Eq.1 in a given Gaussian point are: (a) Determine the maximum normal stress thus the corresponding plane or angle θ_{max}; (b) Calculate the α, the angle between critical plane and crack plane, by equations in Table.1, hence the critical plane angle, $\theta_{max} + \alpha$; (c) Compute the fatigue strengths on crack plane by Tsai-Wu strength transformation. $f_{N_f(\theta_{max})}$, $t_{N_f(\theta_{max})(2)}$ and $t_{N_f(\theta_{max})(3)}$ are the functions of cyclic number *N*, assuming *N* is known in advance; (d) Transform the stress tensor to critical plane to evaluate Eq.1.

2.3 Quasi-static Damage Analysis

2.3.1 Mechanic Properties of the Impregnated Yarn (UD)

Yarns are locally represented as impregnated UD composite, which is considered as transversally isotropic homogeneous material. The averaged fibre volume fraction in the yarn could be obtained from the geometrical model of the reinforcement, which preserves the overall fibre volume fraction in the unit cell.

Yarn stiffness matrix components and Poisson ratios are calculated through Chamis' equations. Another set of properties concern the static damage initiation, the strengths. Since the strengths depend on local Vf which varies from 30% to 90%, not completely covered by existing database, the 'educated guesses' may be adopted [3].

2.3.2 Damage Propagation Law

The damage initiation is captured by Tsai-Wu criterion before fibre breakage (after fibre breakage, the material point is considered to be completely damaged). A material point post-damage behavior is described by an anisotropic damage mode (Table 2). Symbols *L*, *T* and *Z* correspond to longitudinal, transversal and vertical direction to fibre bundles, respectively. *t* and *c* indicate the tension and compression. Mode *L* denotes fibre breakage while other modes denote inter-fibre cracks dominant by corresponding stress components [3,4]. The post-damaged stiffness matrix will be computed (the formulae can be found in [3,4]) based on the damage tensor of the damage mode, identified by the maximum value of the stress-to-strength ratios. Term $\sigma_L^2 / F_L^t F_L^c$ being maximum of all those terms when Tsai-Wu is satisfied would be the criterion for fibre breakage in [3,4]. However, by studying material points of carbon fibre textile composite, it shows that condition leads to pre-mature fibre failure because that term may be still much less than its crucial value 1.0, for instance 0.5. Hence, the term for mode *L* is modified to be larger than 1.0 when fibres start to break.

Table 2. Anisotropic damage mode

Damage mode	Anisotropic damage model for fiber bundle				Isotropic damage model for matrix
	Mode L 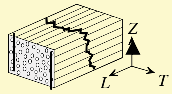	*Mode T & LT* 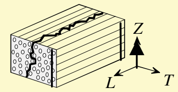	*Mode Z & ZL* 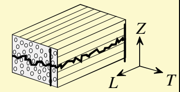	*Mode TZ* 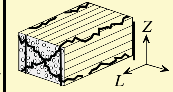	
Maximum stress-to-strength ratio	$\frac{\sigma_L^2}{F_L^t F_L^c}$ >1	$\frac{\sigma_T^2}{F_T^t F_T^c}$ or $\left(\frac{\tau_{LT}}{F_{LT}^s}\right)^2$	$\frac{\sigma_Z^2}{F_Z^t F_Z^c}$ or $\left(\frac{\tau_{ZL}}{F_{ZL}^s}\right)^2$	$\left(\frac{\tau_{TZ}}{F_{TZ}^s}\right)^2$	——
Damage tensor $\begin{bmatrix} D_L & 0 & 0 \\ 0 & D_T & 0 \\ 0 & 0 & D_Z \end{bmatrix}$	$\begin{bmatrix} 1 & 0 & 0 \\ 0 & 0 & 0 \\ 0 & 0 & 0 \end{bmatrix}$	$\begin{bmatrix} 0 & 0 & 0 \\ 0 & 1 & 0 \\ 0 & 0 & 0 \end{bmatrix}$	$\begin{bmatrix} 0 & 0 & 0 \\ 0 & 0 & 0 \\ 0 & 0 & 1 \end{bmatrix}$	$\begin{bmatrix} 0 & 0 & 0 \\ 0 & 1 & 0 \\ 0 & 0 & 1 \end{bmatrix}$	$\begin{bmatrix} 1 & 0 & 0 \\ 0 & 1 & 0 \\ 0 & 0 & 1 \end{bmatrix}$

2.3.3 Validation of the Static Damage Algorithm

The comparison of the computed results and experimental data for PW12K-CFRP is listed in Table.3. The experimental data is extracted from literature [9] and the geometry is produced by the WiseTex software [11] with the following parameters of the reinforcement as shown in Table 3.

The parameters of the fibres and the matrix and strength parameters of the impregnated yarns used in the calculation were obtained from [5]. One unit cell with periodic boundary conditions in the three directions was modelled in FE simulation.

Table 3. Material properties of PW12K-CFRP through evaluation and experiment

	Fibre in yarn	Yarn width (mm)	Yarn Thickness (mm)	Ends/picks count, 1/cm		Total Vf	E11 (GPa)	Tensile Strength (MPa)	Ultimate Strain (%)
Input data	12K	4	0.15	2.40	Exp. Data [**9**]	50.5%	61	807MPa	1.3
					Finite elements	50.8%	64	880MPa	1.4

The virtual tensile test along warp direction is applied to a UC. The program will determine the strain value where first damage occurs, which is damage initiation strain named ε_1. During stretching, transversal cracks are continuously forming, so averaged stiffness is supposed to keep reducing. However, this reduction is hardly observed in experiments. Literature [10] reported this effect so-called stiffening effect, which is also considered in the calculations to compensate the stiffness reduction.

Fig.2 illustrates the computed strain-stress diagram. Damage initiation strain ε_1=0.33 is in reasonable corresponding to the reported values for various carbon/epoxy textile composites [12]. The averaged stiffness and ultimate strain are also consistent to those of experimental data – Table.3.

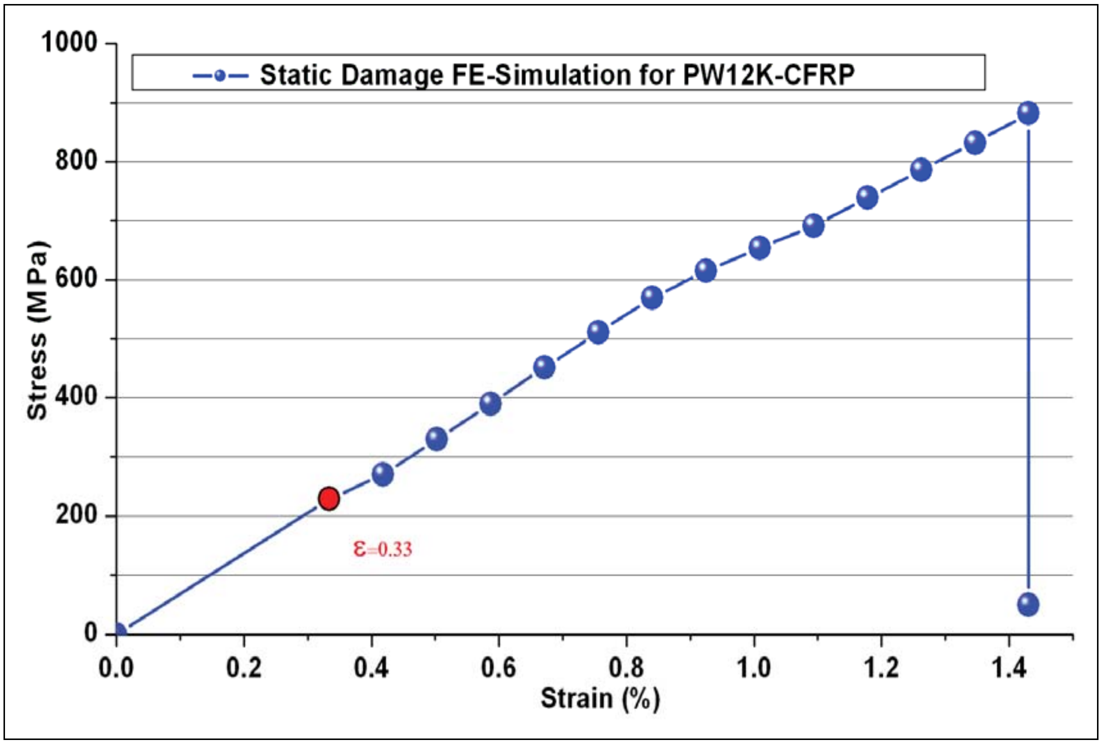

Fig.2 Computed quasi-static strain-stress diagram for PW12K-CFRP

3. IMPLEMENTATION OF THE FATIGUE MODEL

Building of the FE model (Fig.3) starts with geometrical model of the reinforcement, created with the WiseTex software [11]. Further, MeshTex [3] plays a role of mesh generator, correcting also interpenetrations of the yarn volumes. Fig.3b illustrates the mesh in the yarns with 8626 elements, which inherits the structure of geometry from WiseTex.

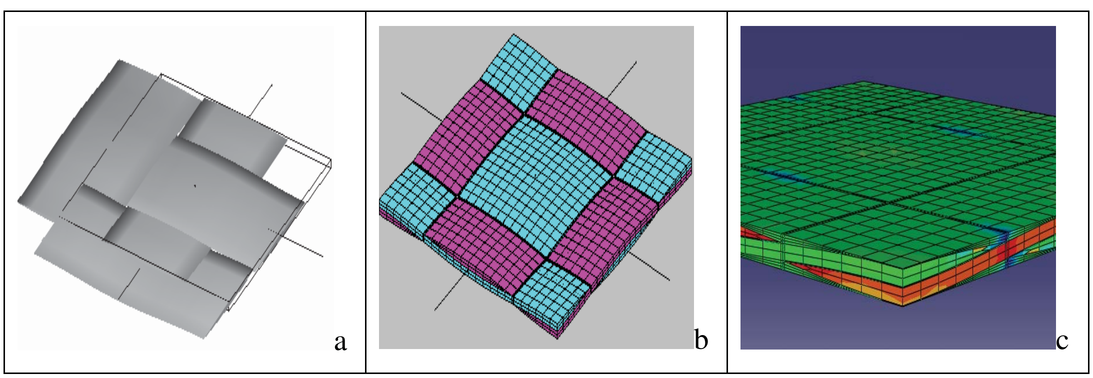

Fig.3 From geometrical model to FE mesh: (a) geometry of PW12K-CFRP from WiseTex; (b) mesh in the yarns from MeshTex (c) right one is the FE model in Abaqus

Abaqus FE code is adopted due to its powerful nonlinearity performance and user defined material behavior: Globally, Python script controls the program flow, encapsulating all the functionalities such as applying PBCs, calling UMAT, calling solver and communicating with database. Locally in every Gaussian point, user defined material behaviors, Tsai-Wu criterion plus anisotropic damage model, is applied in UMAT.

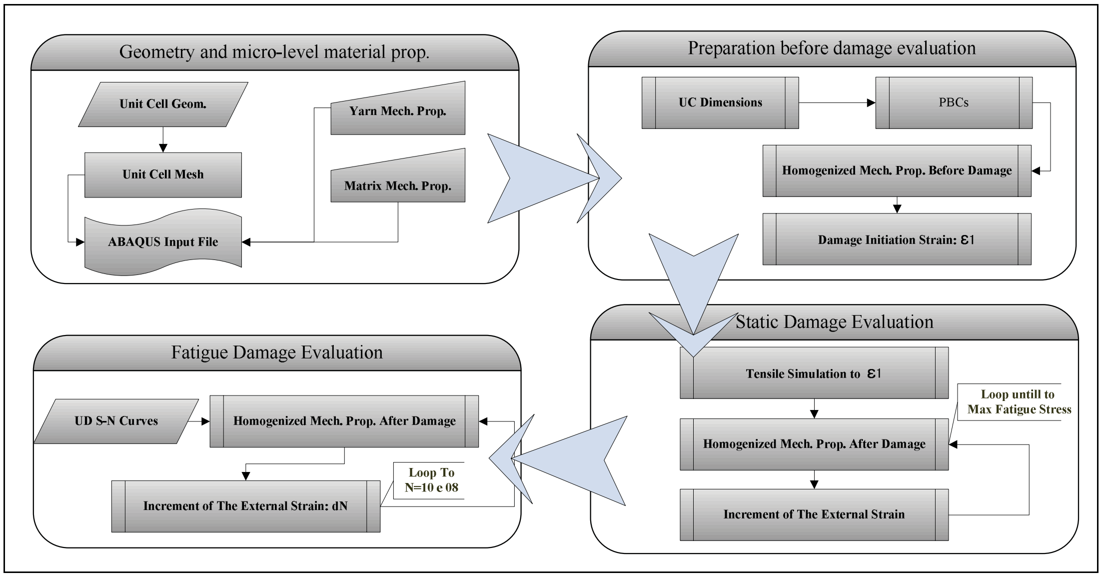

Fig.4 Road map for fatigue evaluation

Fig.4 shows steps in the fatigue modeling: (a) meso-scale FE model preparation, (b) pre-damage properties evaluation, (c) static damage analysis and (d) fatigue damage analysis. Static damage occurs when UC is loaded to maximum fatigue stress. The degraded material properties are afterwards passed to fatigue damage evaluation. In the fatigue analysis, intact material is 'wore out' gradually. Following that, 'sudden damage' takes place due to the stress redistribution.

4. VALIDATION OF THE FATIGUE MODEL

4.1 Materials and Input Data For Modeling

UD properties were completely extracted from paper [5]. The validation material (PW12K-CFRP) properties are listed in Table.3. Besides the basic material properties, this modeling work requires four S-N curves of UD composite, which are S-N curve of fibre direction, transversal fibre direction, in-plane-shear direction and out-of-plane-shear direction. Those data in Fig.5 could also be extracted from paper [5].

For mathematical representation of S-N curves the double logarithmic linear model (DLL, Eq.2) is used — Fig.5. A drawback of DLL is the static strength could not be intergraded very well, which means for the first load cycle the DLL can not predict the fatigue strength accurately. Remedy could be non-linear Bastenaire model. However, Bastenaire model has no reverse function in basic expression, which requires iteration method to compute the fatigue strength when cycle number N is known and fatigue strength unknown.

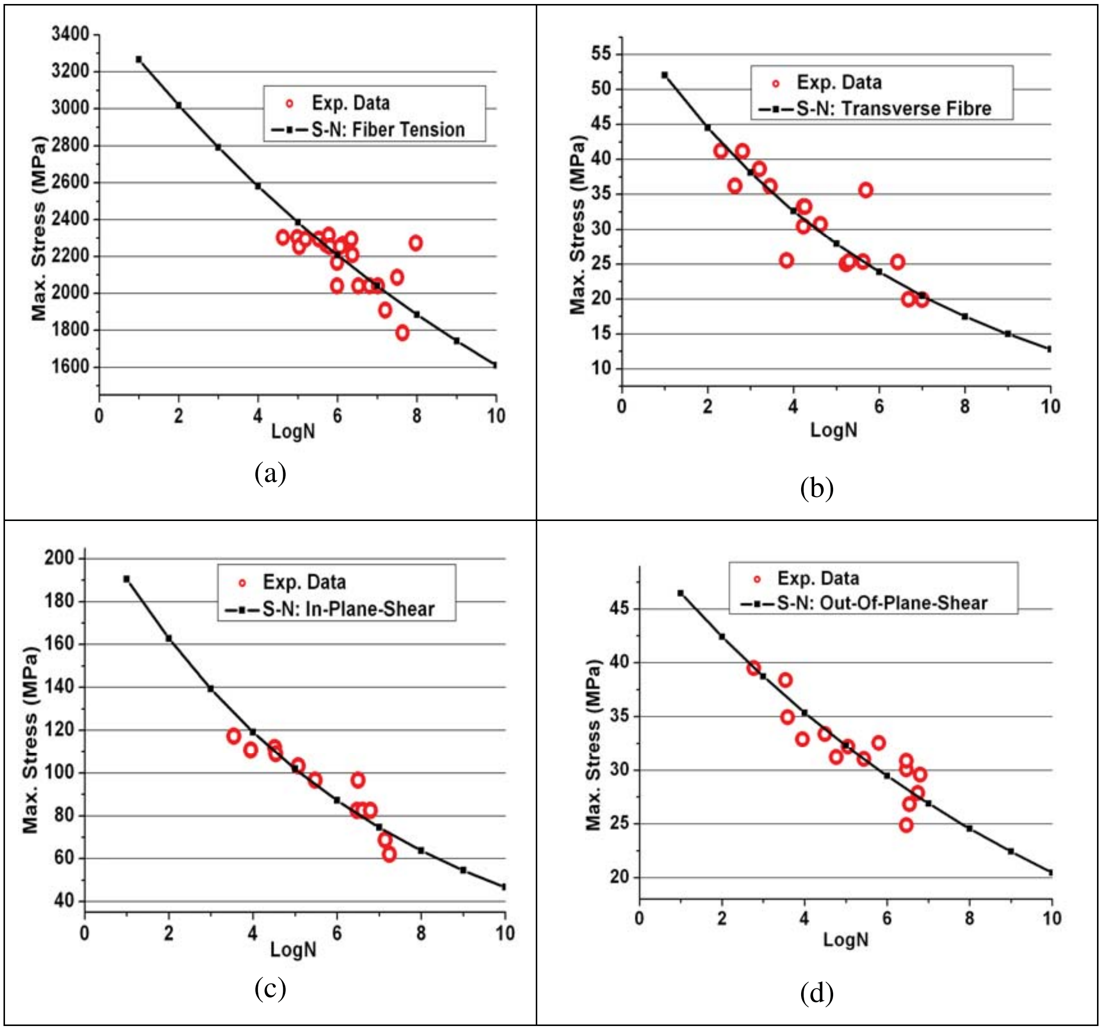

Fig.5 S-N curves as input calculated through double linear logarithm recession: (a)fibre tension; (b) transverse fibre tension; (c) in-plane shear; (d) out-of-plane shear

$$\log_{10} S = -A \log_{10} N + B \quad (2)$$

In Eq.2, S and N stand for fatigue strength and cyclic loading number respectively. A, B, are constant coefficients evaluated by regression method.

4.2 Validation

Agreement between experiments [9] and simulation are shown in Fig.6. Deviation occurs at low-cycle fatigue. Possible reasons are: (a) Geometrical nonlinearity was not taken into account. In experiments, the yarns along to the stretching loading will be flattened on high stress level. High crimp leads to high local tensile stresses and reduces the fatigue life. (2) Final fatigue failure was predicted by the first fibre failure but not by the ratio of reduction of averaged stiffness.

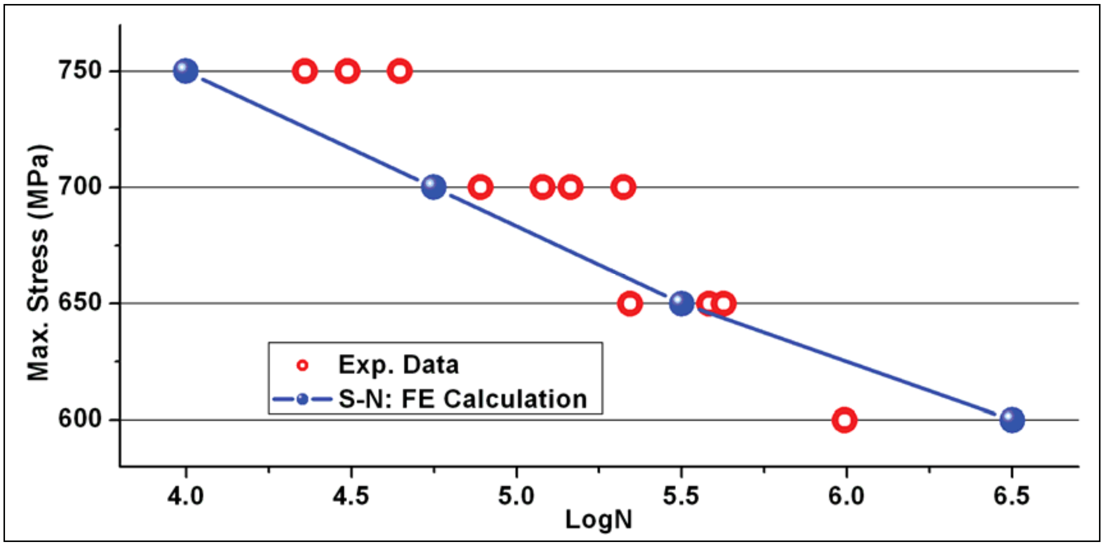

Fig.6 Validation for simulation of fatigue damage evolution and fatigue failure

5. CONCLUSIONS

A promising numerical method for textile composites fatigue analysis is proposed based on meso-scale level with FE method. For static analysis, averaged properties are verified through types of materials and shows good agreements (due to space limit, only PW12K-CFRP explained in this paper). Fatigue analysis also shows satisfactory results compared with experimental data in literature. Elaboration will be carried out on following aspects: (a) Geometrical nonlinearity; (b) Bastenaire recession for input S-N curves; (c) Stiffness degradation curve during fatigue.

ACKNOWLEDGEMENTS

This work is financed by F.W.O. project under the cooperation between the Departments of Metallurgy and Materials Engineering in Katholieke Universiteit Leuven and Department of Materials Science and Engineering in Ghent University. The support from collaborators of both departments and from Mr. Satoshi Hanaki is highly noted.

References

1. S.Hanaki, S.V.Lomov, I.Verpoest, M.Zako, H.Uchida, Estimation of fatigue life for textile composites based on fatigue test for unidirectional materials. Finite element modelling of textiles and textile composites, St-Petersburg, 26-28 Sep. 2007.
2. S.Kari, J. Crookston, A. Jones, N. Warrior, A. Long, Micro and meso scale modelling of mechanical behaviour of 3d woven composites, Proceedings of SEICO 08 SAMPE Europe International Conference, Paris, 2008.
3. Stepan V. Lomov, Dmitry S. Ivanov, Ignaas Verpoest, Masaru Zako, Tetsusei Kurashiki, Hiroaki Nakai, Satoru Hirosawa, Meso-FE modelling of textile composites: Road map, data flow and algorithms, Composites Science and Technology, Volume 67, Issue 9, July 2007, Pages 1870-1891.
4. Zako M, Uetsuji Y, Kurashiki T. Finite element analysis of damaged woven fabric composite materials. Compos Sci Technol 2003; 63:507-16.
5. Shokrieh, Mahmood M., Lessard, Larry B. Progressive Fatigue Damage Modeling of Composite Materials, Part II: Material Characterization and Model Verification, Journal of Composite Materials 2000 34: 1081-1116.
6. Yasuhiro Nishikawa, Kazuya Okubo, Toru Fujii, Kazumasa Kawabe, Fatigue crack constraint in plain-woven CFRP using newly-developed spread tows, International Journal of Fatigue, Volume 28, Issue 10, The Third International Conference on Fatigue of Composites, October 2006, Pages 1248-1253.
7. Yongming Liu, Sankaran Mahadevan, Multiaxial high-cycle fatigue criterion and life prediction for metals, International Journal of Fatigue, Volume 27, Issue 7, July 2005, Pages 790-800.
8. Yongming Liu, Sankaran Mahadevan, A unified multiaxial fatigue damage model for isotropic and anisotropic materials, International Journal of Fatigue, Volume 29, Issue 2, February 2007, Pages 347-359.
9. Yasuhiro Nishikawa, Kazuya Okubo, Toru Fujii, Kazumasa Kawabe, Fatigue crack constraint in plain-woven CFRP using newly-developed spread tows, International Journal of Fatigue, Volume 28, Issue 10, The Third International Conference on Fatigue of Composites, October 2006, Pages 1248-1253.
10. N. Toyama, J. Takatsubo, An investigation of non-linear elastic behavior of CFRP laminates and strain measurement using Lamb waves, Composites Science and Technology, Volume 64, Issue 16, December 2004, Pages 2509-2516.
11. Ignaas Verpoest, Stepan V. Lomov, Virtual textile composites software WiseTex: Integration with micro-mechanical, permeability and structural analysis, Composites Science and Technology, Volume 65, Issues 15-16, 20th Anniversary Special Issue, December 2005, Pages 2563-2574.
12. S.V. Lomov, D.S. Ivanov, T.C. Truong, I. Verpoest, F. Baudry, K. Vanden Bosche, H. Xie, Experimental methodology of study of damage initiation and development in textile composites in uniaxial tensile test, Composites Science and Technology, Volume 68, Issue 12, Deformation and Fracture of Composites: Analytical, Numerical and Experimental Techniques, with regular papers, September 2008, Pages 2340-2349.